Synthesis and Characterization of a Series of (Diphenyldipyrazolylmethane)copper Complexes as Possible Precursors to Type I Blue Copper Protein Active Site Models

Janet L. Shaw,[a] Thomas B. Cardon,[b] Gary A. Lorigan,[b] and Christopher J. Ziegler*[a]

Keywords: Copper / N ligands / Pyrazolylmethanes / Scorpionates

A series of copper complexes employing the neutral, bidentate, pyrazole-based ligand diphenyldipyrazolylmethane was synthesized and fully characterized by various techniques, including elemental analysis, EPR, and structure elucidation by single-crystal X-ray diffraction. The structures of compounds **3**–**8** reveal variable coordination environments at the copper center, ranging from square pyramidal to tetrahedral, depending on the steric bulk at the pyrazole periphery and on the identity of the counterion. Cyclic voltammetry data on these compounds show a positively shifted reduction potential as compared to those observed employing the negatively charged pyrazolylborates or β-diketiminates. These results indicate that these compounds may lead to (thiol)copper complexes that more accurately reproduce the reduction potentials observed during electron-transfer processes in blue copper proteins.

Introduction

Small models of the active sites of metalloenzymes remain important for understanding the structure−function relationships that exist between immediate metal-ion coordination environments and activities such as electron transport or dioxygen activation. Scorpionate ligands, such as the sterically hindered pyrazolylborates (see Figure 1), have been successful in mimicking many of the coordination geometries observed in the active sites of metalloproteins.[1−3] In addition to numerous zinc complexes,[4−6] pyrazolylborates have been employed for generating models of both type I blue copper proteins[7−10] and type III dicopper proteins,[11] such as plastocyanin and hemocyanin, respectively.[12−13] The ease of synthesis, the ability to add additional bulk to the pyrazole moieties, and the favorable multidentate binding mode are all responsible for the continued interest in pyrazolylborates as ligands for small model complexes. However, pyrazolyborates are negatively charged and can lead to complexes with higher oxidation states than those of the metal sites in native proteins.[14] Therefore, work continues toward the development of model complexes that can more accurately model the geometry and electronic structure of metal ions in proteins.

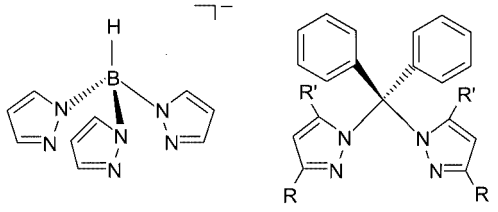

Figure 1. Schematic drawings of the ligands tris(pyrazolyl)borate (left) and diphenyldipyrazolylmethane (right) where R = R′ = H (**1**), R = R′ = CH_3 (**2**) and R = CH_3, R′ = H (**3**)

We have begun to explore the synthesis of active site models for copper proteins using the ligand diphenyldipyrazolylmethane, shown in Figure 1. Synthesized previously for use in polymerization catalysis,[15−16] this ligand is neutral and contains two pyrazole moieties available for bidentate metal-ion coordination. Like the pyrazolylborates, the pyrazole rings may be functionalized to incorporate more steric bulk around the copper center. This can be exploited to enforce desired geometries, inhibit the formation of bridging species, or promote low-coordination-number end products. Once synthesized, these compounds may be useful as starting materials in reactions with thiol or carboxylate-containing ligands to produce small model complexes of copper-enzyme active sites. Since these models incorporate a neutral ligand, we believe that they will exhibit redox potentials that more closely resemble those observed in nature

[a] University of Akron, Department of Chemistry, Akron, OH 44325, U.S.A.
Fax: (internat.) +1-330-972-7370
E-mail: ziegler@uakron.edu
[b] Miami University, Department of Chemistry, Oxford, OH 45056, U.S.A.
Supporting information for this article is available on the WWW under http://www.eurjic.org or from the author.

for type I blue copper proteins. Here we report our results on the synthesis and characterization of some (diphenyldipyrazolylmethane)copper complexes including crystal structures, cyclic voltammetry, and electron paramagnetic resonance spectra. We observe high potentials for the Cu^{II}/Cu^{I} redox couple, and increased steric bulk at the periphery of the pyrazole ring enforces lower coordination numbers.

Results and Discussion

The diphenyldipyrazolylmethanes (Figure 1, right) were synthesized using a modified procedure reported by Trofimenko that involves the generation of a pyrazolide ion and subsequent reaction with a dihalomethane.[17] These ligands have previously been employed in molybdenum[15] and palladium[16] complexes for use as catalysts. Figure 2 shows the crystal structures elucidated for ligands **1** and **2**. The C(1)−N(1,3) bond lengths in **1** are 1.490(4) Å and 1.484(4) Å, respectively, while in **2** they are 1.4753(17) Å and 1.4754(16) Å. The angle formed by N3−C1−N1 in **1** is 108.0(2)°, while in **2** it is 104.85(10)°. Based on their structural characteristics, these ligands should act as bidentate chelators. A comparison of the bond angles and lengths for these two ligands can be found in Table 1.

The copper complexes were synthesized by a reaction of either copper(II) nitrate or copper(I) chloride with the appropriate ligand in a number of organic solvents. In most cases the final product remained soluble throughout the reaction and was isolated by recrystallization from the appropriate solvent. All reactions produce X-ray quality crystals with little purification required.

A survey of the literature uncovers few examples of 1:1 complexes forming between dipyrazolyalkanes and either copper(I) or copper(II),[18−21] with the preference instead being 2:1 ligand-to-metal complexation.[22−23] Of these, less crystallographic information is available and the compounds have instead been characterized by other techniques such as IR spectroscopy, magnetic susceptibility, EPR, and ^{1}H NMR spectroscopy. The stoichiometry of the observed final products in the literature appears to depend on the starting copper salt (chloride salt vs. nitrate salt) and the degree of steric hindrance at the pyrazole periphery.

Unlike in the dipyrazolylalkane complexes, the majority of the compounds reported here form 1:1 complexes. The geometries of compounds **4**−**8** range from square pyramidal to tetrahedral, depending on the steric bulk at the pyrazole periphery and the counterion identity. Table 2 and Table 3 present relevant bond lengths and angles and the crystallographic data for compounds **4**−**8**, respectively. Compound **4** (see Figure 3) is best described as having a distorted square-pyramidal geometry. The copper(II) center is ligated by one bidentate **1** ligand, two nitrates and one water molecule in the axial position. The methanol employed in this reaction was not dried prior to use, and the

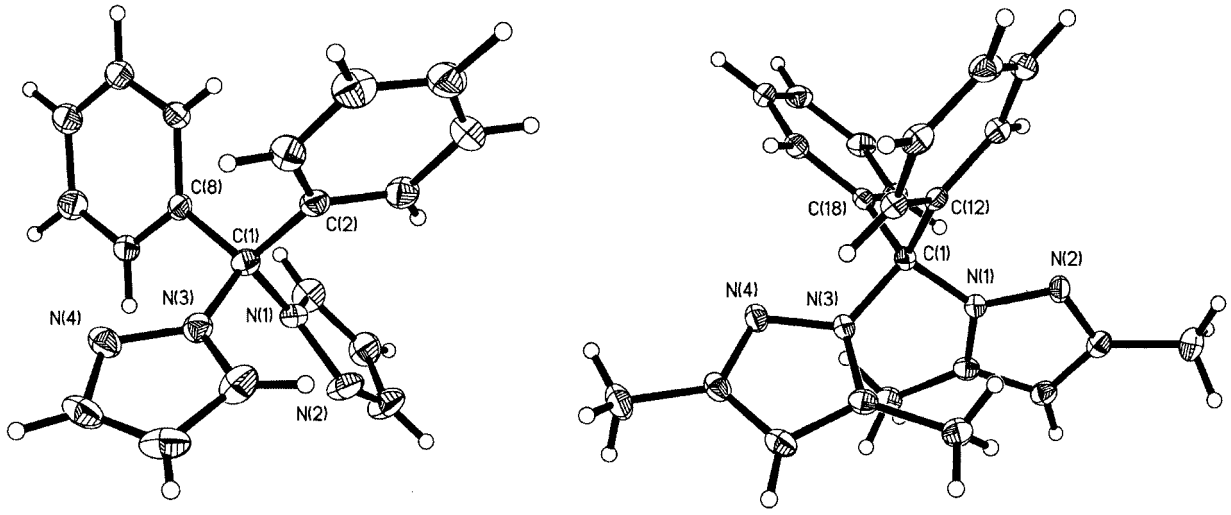

Figure 2. Structures of compounds **1** and **2** with thermal ellipsoids drawn at 50 % probability

Table 1. Comparison of bond lengths (Å) and angles (°) in **1** and **2**

	1		**2**	
C−N	C1−N1 1.490(4)	C1−N3 1.484(4)	C1−N1 1.4753(17)	C1−N3 1.4754(16)
C−C	C1−C2 1.535(4)	C1−C8 1.521(4)	C1−C12 1.5459(18)	C1−C18 1.5455(18)
N−C−N	N1−C1−N3 108.0(2)		N1−C1−N3 104.85(10)	
C−C−C	C2−C1−C8 113.3(3)		C12−C1−C18 107.26(10)	
N−C−C	N1−C1−C2 109.0(2)	N3−C1−C2 108.6(3)	N1−C1−C12 112.68(10)	N3−C1−C12 109.53(10)

ligated water molecule may have come from residual water in the reaction solvent. The nitrates bind in a monodentate fashion with Cu−O distances of 1.971(3) Å and 1.975(3) Å. Within the literature, the modes of nitrate bonding can vary. For example, in the similar compound $Cu(bmpp)(NO_3)_2$ the two nitrates coordinate to the copper in an unsymmetrical bidentate fashion with Cu−O distances of 2.026(2) Å.[24] The Cu−O distance for the coordinating water molecule is 2.256(4) Å and the Cu−N bond lengths are both around 1.986(4) Å.

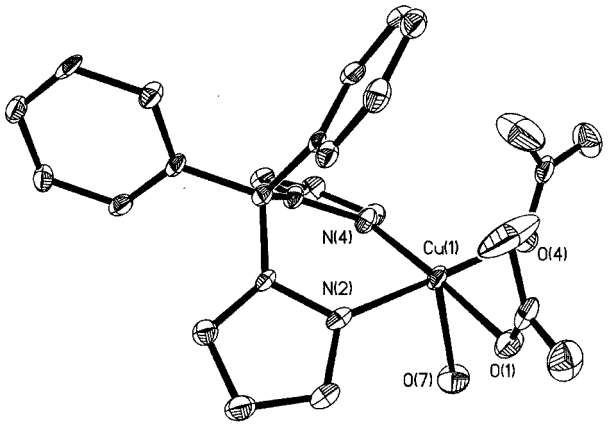

Figure 3. Structure of compound **4** with hydrogens omitted for clarity and thermal ellipsoids drawn at 50 % probability

Compound **5** (Figure 4) exhibits a similar geometry to complex **4**, but the water molecule in the coordination sphere is absent and one of the nitrates binds in a bidentate fashion with Cu−O distances of 1.9959(16) Å and 2.0110(19) Å. These distances are somewhat longer than those seen in **4** for the nitrates bound in a monodentate fashion. The lack of a coordinating water molecule may be due to the increase in steric bulk at the 3 position of the pyrazole ring in **5**. The coordination sphere of **5** is completed with a bidentate **3** ligand [Cu−N4 1.9344(18) and Cu−N2 1.9610(18)] and one monodentate nitrate group [Cu−O1 2.1361(17) Å]. Increasing the steric bulk at the pyrazole periphery in compound **5** alters the geometry from square pyramidal to pseudotetrahedral. In addition, the coordination geometry at the copper center is affected by the binding mode of the nitrate counterion. Whereas in compound **4** both nitrates ligate in a monodentate fashion, in compound **5** one nitrate is bidentate and the other is monodentate. This variable coordination mode of the nitrate counterion is not uncommon.

Unlike the Cu^{II} compounds, the Cu^{I} compound **7**, shown in Figure 5, forms a product with a 2:1 ratio of ligand to metal ion. The copper ion is in a distorted tetrahedral environment with two bidentate **1** ligands with Cu−N distances ranging from 2.007(3) Å to 2.045(3) Å and with N−Cu−N angles ranging from 91.38(10)° to 128.05(10)°. The intraligand N−Cu−N angles are closer to 90° while the interligand N−Cu−N angles are both near 120°. The bond lengths compare nicely to those reported for other 2:1 complexes $[Cu(bpp)_2](BF_4)$ (about 2.031 Å)[23] and $[CuL_2](ClO_4)$ (about 2.037 Å), where L = bis[2,2′-bis(2-imidazolyl)-biphenyl].[25] The bond angles in compound **7** show a slight compression along the intraligand axes. These bond angles compare well with those observed in the copper(II) complexes α- and β-$[Cu(bpp)_2](BF_4)_2$ (95.23−127.20° and 91.34−135.66°, respectively).[23] It is unclear as to why **7** exists as a 2:1 complex, but similar results have been observed in the literature: the ligand-to-metal ratio was found to depend not only on the steric bulk at the pyrazole periphery but also on the identity of the counterion.[21,26]

Table 2. Comparison of bond lengths (Å) and angles (°) in compounds **4**−**8**

	4	**5**	**6**	**7**	**8**
Cu−N	Cu−N2 1.985(4) Cu−N4 1.986(4)	Cu−N2 1.9610(18) Cu−N4 1.9344(18)	Cu−N1 2.008(5) Cu−N3 1.978(5) Cu−N5 1.991(5)	Cu−N2 2.032(3) Cu−N4 2.007(3) Cu−N5 2.045(3) Cu−N7 2.007(3)	Cu−N2 1.961(4) Cu−N4 2.011(4)
Cu−X	Cu−O1 1.975(3) Cu−O4 1.971(3) Cu−O7 2.256(4)	Cu−O1 2.1361(17) Cu−O4 1.9959(16) Cu−O5 2.0110(19)	Cu−O2 2.310(5) Cu−O4 2.025(4)		Cu−Cl1 2.2071(15) Cu−Cl2 2.2388(16)
N−Cu−N	N2−Cu−N4 87.59(15)	N2−Cu−N4 90.25(8)	N1−Cu−N3 92.10(2) N3−Cu−N5 89.9(2) N1−Cu−N5 176.1(2)	N2−Cu−N4 91.38(10) N5−Cu−N7 91.54(10) N2−Cu−N5 105.03(9) N4−Cu−N7 119.18(8) N2−Cu−N7 124.26(10) N4−Cu−N5 128.05(10)	N2−Cu−N4 88.72(16)
X−Cu−X	O4−Cu−O1 93.53(15) O4−Cu−O7 82.03(15) O1−Cu−O7 81.85(16)	O4−Cu−O5 64.12(7) O4−Cu−O1 105.44(7) O1−Cu−O5 105.00(7)	O2−Cu−O4 84.84(15) O4−Cu−N1 85.55(17)		Cl1−Cu−Cl2 95.82(6)
X−Cu−N	O4−Cu−N2 176.82(16) O1−Cu−N4 176.71(16) O1−Cu−N2 89.33(15) O4−Cu−N4 89.53(15) O7−Cu−N2 97.00(16) O7−Cu−N4 97.37(16)	O4−Cu−N2 101.43(7) O5−Cu−N2 158.02(8) O1−Cu−N2 94.59(7) O1−Cu−N4 96.42(7) O4−Cu−N4 154.12(7) O5−Cu−N4 97.23(7)	O2−Cu−N1 88.39(17) O4−Cu−N3 170.72(19) O4−Cu−N5 91.95(18) O2−Cu−N3 104.08(17) O2−Cu−N5 94.33(18)		Cl1−Cu−N2 153.42(13) Cl1−Cu−N4 95.66(12) Cl2−Cu−N2 91.36(12) Cl2−Cu−N4 153.99(12)

Table 3. Crystallographic data for compounds **1**−**2** and **4**−**8**.

	1	**2**	**4**	**5**	**6**	**7**	**8**
Molecular formula	$C_{19}H_{16}N_4$	$C_{23}H_{24}N_4$	$C_{19}H_{18}CuN_6O_7$	$C_{21}H_{20}CuN_6O_6$	$C_{15}H_{24}CuN_8O_6$	$C_{38}H_{32}N_8Cl_2Cu_2$	$C_{19}H_{16}Cl_2CuN_4$
Fw	300.36	356.46	505.93	515.97	475.96	798.70	434.80
Crystal system	Ortho-rhombic	Monoclinic	Monoclinic	Orthorhombic	Orthorhombic	Monoclinic	Triclinic
Space group	*Pna*2$_1$	*P*2$_1$/*n*	*P*2$_1$/*n*	*P*2$_1$2$_1$2$_1$	Pbca	*Cc*	$P\bar{1}$
Cell constants							
a (Å)	14.857(5)	10.5405(11)	10.1001(15)	8.7650(8)	12.488(3)	21.0687(15)	7.461(3)
b (Å)	14.343(5)	10.5904(11)	12.7917(19)	9.4840(9)	11.531(3)	11.5004(8)	9.126(3)
c (Å)	7.113(2)	16.9489(18)	15.494(2)	26.280(2)	29.564(7)	17.2606(12)	13.938(5)
α (deg)	90	90	90	90	90	90	81.098(7)
β (deg)	90	93.549(2)	90.176(2)	90	90	115.806(10)	76.729(7)
γ (deg)	90	90	90	90	90	90	89.966(7)
Z	4	4	5	4	8	4	2
V (Å^3)	1515.8(9)	1888.3(3)	2001.8(5)	2184.6(4)	4257.1(17)	3765.1(5)	912.0(6)
Abs. coeff. μ_{calc} (mm^{-1})	0.081	0.076	1.437	1.052	1.075	1.310	1.501
δ_{calc} (Mg/m^3)	1.316	1.254	2.098	1.569	1.485	1.409	1.583
F(000)	632	760	1295	1060	1976	1632	442
Cryst. dimens. (mm)	0.2 × 0.1 × 0.05	0.3 × 0.2 × 0.05	0.4 × 0.1 × 0.1	0.4 × 0.3 × 0.2	0.1 × 0.03 × 0.03	0.1 × 0.2 × 0.2	0.1 × 0.1 × 0.05
No. of reflcns. collcd.	12699	16284	16932	18485	34627	16313	6670
No. of unique reflcns.	3612	4468	4651	5198	5131	8483	3185
No. of params.	272	340	370	387	289	451	299
R(*F*)	0.0702	0.0469	0.0723	0.0325	0.1180	0.0383	0.0576
$R_w(F^2)$	0.1317	0.1044	0.1321	0.0739	0.1786	0.0919	0.1020
GOF	1.035	1.044	1.267	1.074	1.280	1.033	1.037
Ratio min/max trans.	0.730155	0.906570	0.632826	0.776535	0.460436	0.892294	0.826543

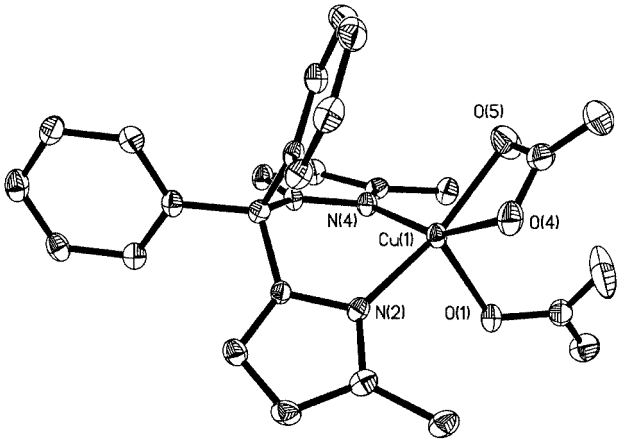

Figure 4. Structure of compound **5** with hydrogens omitted for clarity and thermal ellipsoids drawn at 50 % probability

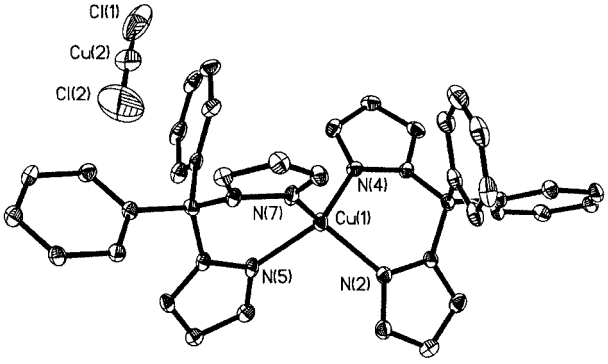

Figure 5. Structure of compound **7** with hydrogens omitted for clarity and thermal ellipsoids drawn at 50 % probability

Exposing an acetonitrile solution of compound **7** to air causes the clear solution to turn green over a 12 hour period. This color change is due to the oxidation of the d^{10} copper(I) compound (**7**) to the d^9 copper(II) compound (**8**). Crystals of the green solid **8** (see Figure 6) were grown from the air-exposed product by layering a solution of CH_2Cl_2 with hexane at room temperature. The crystal structure was elucidated and was found to contain a Cu^{II} ion in a tetrahedral-coordination environment with one bidentate **1** ligand and two ligated chloride ions. The average Cu−N and Cu−Cl bond lengths are 1.986(4) Å and 2.223(16) Å, respectively. These lengths are in close agreement with those reported for the tetrahedral complex Cu(bdpp)Cl_2, where bdpp is 1,3-bis(3′,5′-dimethylpyrazol-1′-yl)propane.[24] The N−Cu−N bond angle is 88.72(16)° and the N−Cu−Cl bond angles range from 91.36(12)−153.99(12)°, thus exhibiting a distorted tetrahedral environment at the copper center.

Unlike in the synthesis of compounds **4**−**8**, something unanticipated occurs upon reacting **2** with copper nitrate: the ligand decomposes. The product that forms (compound **6**) is a five-coordinate, distorted, square-pyramidal copper(II) complex with three ligating 3,5-dimethylpyrazole moieties and two monodentate nitrates (Figure 7). Relevant bond angles and lengths are listed in Table 2. The Cu−N bond-length values compare nicely to those reported for the polymeric $[Cu(pyrazole)_2]_x$ complex [1.992(6) Å vs. 1.957(2) Å].[27]

Similar examples have been documented in the literature for the decomposition of pyrazole-based ligands upon reac-

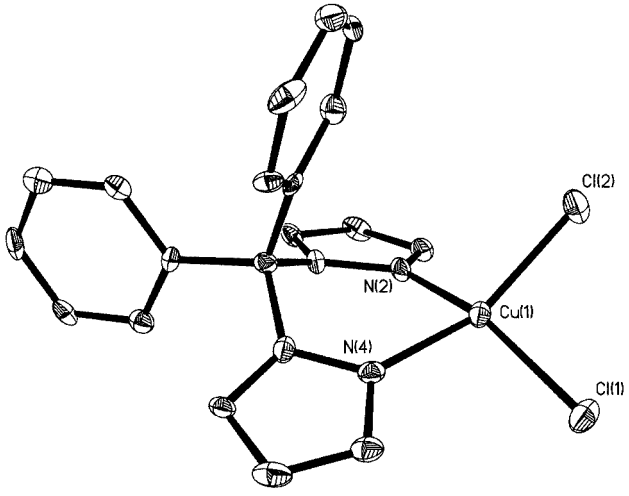

Figure 6. Structure of compound **8** with hydrogens omitted for clarity and thermal ellipsoids drawn at 50 % probability

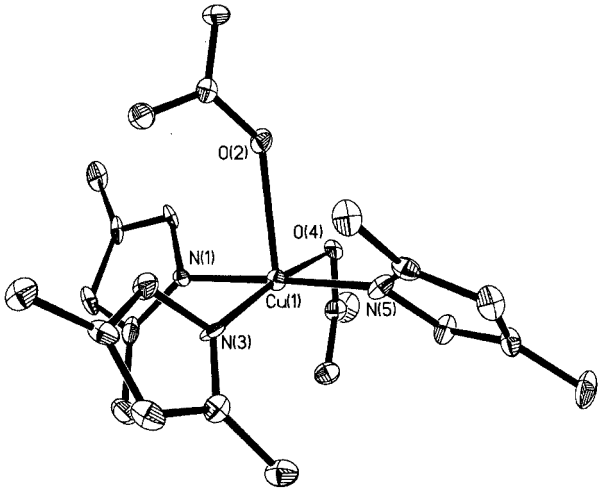

Figure 7. Structure of compound **6** with hydrogens omitted for clarity and thermal ellipsoids drawn at 50 % probability

tion with metal salts.[28,29] The proposed mechanism involves metal-mediated cleavage of the pyrazole nitrogen−X bond, where X may be boron, as is the case with pyrazolylborates, or carbon, as is the case in this report. We do not believe that compound **6** is a product of pyrazole impurity from the previous ligand synthesis because complete characterization of the Pz''_2CPh_2 ligand, prior to use in this metallation reaction, indicates purity. Attempts are currently under way to synthesize the $Cu(Pz''_2CPh_2)$ derivative under anaerobic conditions using dry solvents.

The low-temperature solution state EPR spectra of compounds **4**, **5**, **6** and **8** are shown in Figure 8. Changes in the features of such spectra result from the coordinated ligands, the compound geometry, and the compound charge, in decreasing order of importance.[30,31] Because the ligands used here are nearly identical, varying only by one methyl substituent, and because the coordination geometry of each complex is similar, as seen in Figures 3 4, 5 and 6, one would expect little change in the EPR spectrum of each compound, as is seen in Figure 8. Calculated $g_{\|}$, $g\perp$ and $A_{\|}$ values are shown in Table 4 and these values are similar to those recorded in the literature for compounds with similar structures.[24,32−34] The hyperfine splitting pattern for a Cu 3/2 spin is observed but there are no observable superhyperfine interactions. Calculated $A_{\|}$ values for **5** reveal a slight compression in this region of the spectra.

Table 4. Selected EPR parameters for **4**, **5**, **6** and **8**

	$g_{\|}$	$g_{\perp}$	$A_{\|}$
4	2.492	2.074	160 G
5	2.312	2.079	149 G
6	2.298	2.063	158 G
8	2.287	2.068	164 G

The cyclic voltammogram of **4** is shown in Figure 9. The quasi-reversible wave at 0.55 V vs. SCE (E_{pc} at 0.48 V, E_{pa} at 0.62 V, 0.31 V vs. NHE) is attributed to the Cu^{II}/Cu^{I} redox couple. A scan rate of 50 mv/s afforded optimal reversible behavior. A cyclic voltammogram was also acquired for compound **5** and is shown in Figure 9. The reversible wave at 0.63 V vs. SCE (E_{pc} at 0.55 V, and E_{pa} at 0.71 V, 0.39 V vs. NHE) is also ascribed to the Cu^{II}/Cu^{I} redox pair and is shifted by +0.1 V as compared to that observed for **4**. Once again, the best spectra resulted when

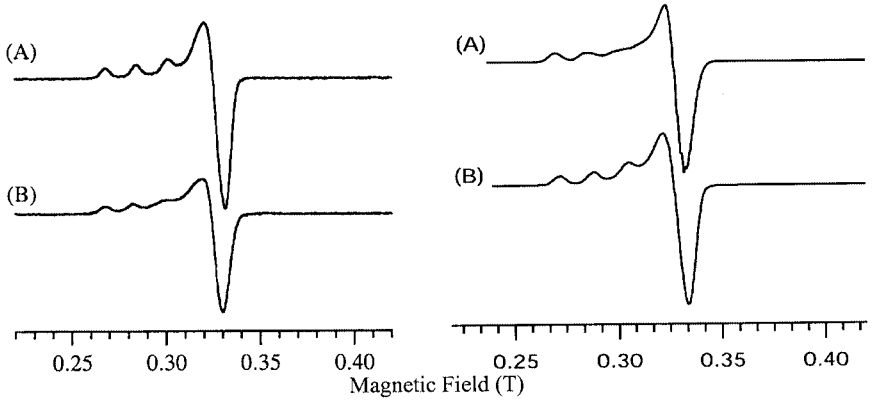

Figure 8. EPR spectra of compounds **4** (top, left), **5** (bottom, left), **6** (top, right) and **8** (bottom, right) (9.42 GHz) in MeOH at 120 K

a scan rate of 50 mv/s was used. Altering this scan speed resulted in a decreased intensity of the voltammogram half-wave features.

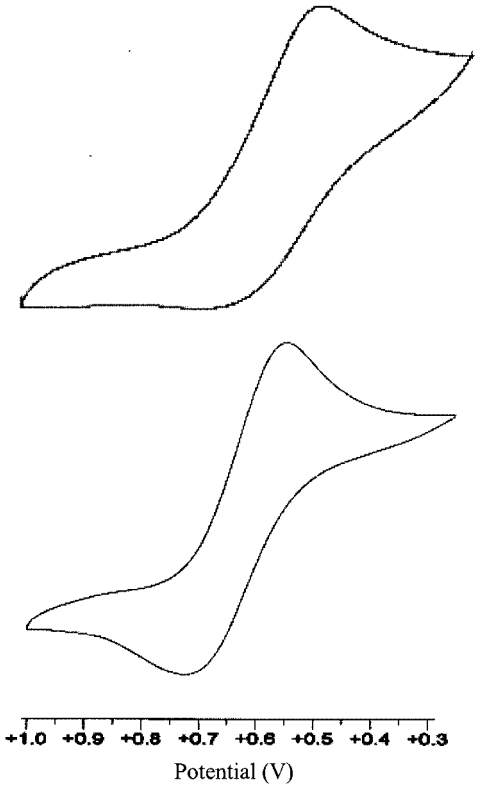

Figure 9. Cyclic voltammograms of compounds **4** (top) and **5** (bottom) at a scan rate of 50 mV/s in CH_3CN with 0.1 M $[Bu_4N]BF_4$ vs. SCE; y-axis is current measured in uA

These potentials are more positive than those of other copper-model complexes in the literature. For instance, in the β-diketiminate copper complex, LCuCl, where L is 2,4-bis(2,6-diisopropylphenylimido)pentane, a half-potential of −0.78 V vs. ferrocene (0.02 V vs. NHE) was reported in CH_2Cl_2.[33] This shift to a more negative potential results, in part, from the negative charge on the diketiminate ligand. The charge shifts the preference toward a +2 oxidation state at the copper center, thus resulting in a more negative potential for the Cu^{II}/Cu^{I} redox couple. Subsequent thiol complexes that incorporate either the above mentioned β-diketiminate or the popular tris(pyrazolyl)borate ligands also have reduction potentials that are significantly lower than those observed in copper-active sites in biology.[7,14]

Attempts were made to isolate thiol complexes by reacting complexes **3** and **4** with bulky aryl thiols such as triphenylmethanethiol or bidentate thiols such as 1,2-benzenedithiol. Each time decomposition occurs forming a reduced metal compound, indicative of colorless copper(I), and the disulfide. A reaction of compound **5** with 1,2-benzenedithiol did lead to a stable green complex in DMF, but crystals were not of X-ray quality. Further work is being done to determine the identity of this product. In addition, attempts are currently under way to further protect the copper ion from reduction chemistry, by increasing the steric bulk at the pyrazole periphery from a methyl to a *tert*-butyl group.

Conclusion

Diphenyldipyrazolylmethane reacts with commercially available copper salts to form low-coordination-number copper complexes. Reactions with copper(II) nitrate produce 1:1 complexes, while the reaction with copper(I) chloride yields a 2:1 complex. Similar compounds presented in the literature, employing dipyrazolylalkanes, produce mainly 2:1 complexes and it is therefore believed that the phenyl rings employed here provide additional protection to the copper ion. Also, the ability of the nitrate counterion to coordinate in different modes (monodentate or bidentate) influences the coordination environment of the copper ion. Additional counterions may be studied in order to affect changes in the copper ion-coordination environment. The geometry of these compounds in the solution state can be further studied by performing conductivity experiments in alcoholic solutions.

We hope that the diphenyldipyrazolyl ligands will produce more biologically relevant model complexes than those that currently exist in the literature because the neutrality of our ligand produces copper complexes with more positive reduction potentials than those observed employing negatively charged ligands, such as the pyrazolylborates. We find that increasing the steric bulk on the pyrazole ring, from compound **4** to compound **5**, leads to a slight preference for copper(I) rather than copper(II), based on the reduction potentials, because of the nearly tetrahedral geometry supported by this ligand. A delicate balance between these two oxidation states is necessary in order to adequately replicate the redox behavior observed in biology in type I blue copper proteins.

Experimental Section

All solvents and starting materials were obtained from commercially available sources and were used without further purification. Mass spectra were recorded using an ES MS Bruker Esquire-LC ion-trap mass spectrometer. ^{1}H NMR spectra were measured on a Gemini 300 MHz spectrometer. The elemental analysis was performed on a CE440 analyzer at the School of Chemical Sciences Microanalysis Laboratory at the University of Illinois at Urbana-Champaign. EPR data were collected at the University of Miami in Ohio. UV/Visible spectra were obtained using a Hitachi U-3010 instrument.

Synthesis of Diphenyldipyrazolylmethane Pz_2CPh_2 (1): All three ligands were synthesized using a slight modification of the procedure by Trofimenko.[17] After isolation of the yellow solid, the ligand was washed with hexanes to yield 1.13 g of white solid (47.7 % yield). Recrystallization by slow evaporation of a saturated toluene solution yielded crystals suitable for single-crystal X-ray diffraction. ^{1}H NMR (300 MHz, $CDCl_3$, 25 °C): δ = 7.65 (d, 2 H, 3-pz), 7.52 (d, 2 H, 5-pz), 7.43−7.33 (m, 6 H, ph), 7.06−7.03 (m, 4 H, ph), 6.31 (dd, 2 H, 4-pz). ES MS (+ ion, MeOH) 323.1 *m*/*z* [M +

Na]. $C_{19}H_{16}N_4$ (300.36): calcd. C 75.97, H 5.38, N 18.64; found C 75.04, H 5.30, N 18.20.

Synthesis of Diphenylbis(3,5-dimethylpyrazolyl)methane Pz''_2CPh_2 (2): Ligand **2** was prepared similarly to ligand **1**. After workup, 1.06 g of yellow solid (43.0 % yield) were obtained. Crystals suitable for X-ray structural elucidation were grown from a THF/CH_3CN solvent mixture. ^1H NMR (300 MHz, $CDCl_3$, 25 °C): δ = 7.30−7.20 (m, 6 H, ph), 7.05−6.95 (m, 4 H, ph), 6.01 (s, 2 H, 4-pz), 2.22 (s, 6 H, 3-methyl), 1.58 (s, 6 H, 5-methyl). ES MS (+ ion, $CHCl_3$/MeOH) 379.2 *m*/*z* [M + Na]. $C_{23}H_{24}N_4$ (356.46): calcd. C 77.49, H 6.80, N 15.71; found C 77.04, H 6.75, N 15.45.

Synthesis of Diphenylbis(3-methylpyrazolyl)methane Pz'_2CPh_2 (3): Ligand **3** was prepared similarly to ligands **1** and **2**. The resulting yellow-orange solution was filtered and reduced under vacuum to afford a yellow oil. Hexanes were added to precipitate out a small amount of brown solid. A yellow solid resulted upon evaporation of the hexanes. This was washed with hexanes and deionized water to yield 1.70 g of a light yellow solid (58.7 %). ^1H NMR (300 MHz, $CDCl_3$, 25 °C): δ = 7.4 (s, 2 H, 5-pz), 7.4−7.3 (m, 6 H, ph), 7.2−7.1 (m, 4 H, ph), 6.05 (d, 2 H, 4-pz), 2.3 (s, 6 H, 3-methyl). ES MS (+ ion, $CHCl_3$/MeOH) 351.2 *m*/*z* [M + Na]. $C_{21}H_{20}N_4$ (328.41): calcd. C 76.80, H 6.15, N 17.05; found C 76.79, H 6.17, N 16.43.

Synthesis of $Cu(Pz_2CPh_2)(NO_3)_2\ H_2O$ (4): $Cu(NO_3)_2$ (0.082 g, 0.44 mmol) in MeOH (10 mL) was combined with a methanol solution of **1** (0.131 g, 0.44 mmol). The blue copper solution darkened upon combining the two reagents. The reaction was allowed to stir for 2 hours at room temperature. This solution was then reduced under vacuum to yield a blue solid. Recrystallization by layering of CH_2Cl_2 and hexane at −42 °C yielded crystals suitable for single-crystal X-ray diffraction (79.1 % yield). UV/Vis (CH_2Cl_2), λ (ε) = 716.0 nm (68 $M^{-1}cm^{-1}$). ES MS (+ ion, MeOH) 425.0 *m*/*z* [M − NO_3]. $C_{19}H_{16}CuN_6O_6$ (505.93): calcd. C 46.77, H 3.31, N 17.22; found C 46.38, H 3.18, N 16.85. $E_{1/2}$ (CH_3CN) 0.55 V vs. SCE (E_{pc} at 0.48 V, E_{pa} at 0.62 V).

Synthesis of $Cu(Pz'_2CPh_2)(NO_3)_2$ (5): $Cu(NO_3)_2$ (0.106 g, 0.56 mmol) dissolved in THF (10 mL) was added to a solution of **3** (0.185 g, 0.56 mmol) in THF (10 mL). The resulting green solution was stirred for 2 hours at room temperature. This solution was then reduced under vacuum to yield a green-blue solid. Crystals were obtained by layering CH_2Cl_2 with hexane at room temperature (75.3 % yield). Two crystal morphologies of this compound formed: blue needles that do not diffract X-rays well, and green blocks that were suitable for single-crystal X-ray diffraction. UV/Vis (CH_2Cl_2), λ (ε) = 779.0 nm (70 $M^{-1}cm^{-1}$). ES MS (+ ion, THF/MeOH) 453.0 *m*/*z* [M − NO_3]. $C_{21}H_{20}CuN_6O_6$ (515.97): calcd. C 48.89, H 3.92, N 16.28; found C 49.61, H 4.11, N 15.94. $E_{1/2}$ (CH_3CN) 0.63 V vs. SCE (E_{pc} at 0.55 V, and E_{pa} at 0.71 V).

Synthesis of $Cu(Pz'')_3(NO_3)_2$ (6): $Cu(NO_3)_2$ (0.264 g, 1.4 mmol) in MeOH (10 mL) was combined with a methanol solution of **2** (0.501 g, 1.4 mmol). The ligand was only partially soluble in methanol. The murky reaction was stirred for 12 hours and then allowed to evaporate down to afford a bluish-green solid. The solid was redissolved in CH_2Cl_2 and filtered to yield two products: a green solid and a blue solid (63.2 % yield crude product). Crystals of the blue solid were grown by layering CH_2Cl_2 and hexane at −42 °C. UV/Vis (CH_2Cl_2), λ (ε) = 633.0 nm (56 $M^{-1}cm^{-1}$). ES MS (+ ion, THF/MeOH) 317.1 *m*/*z* [M − NO_3 − Pz″]. $C_{15}H_{24}CuN_8O_6$ (475.96): calcd. C 37.86, H 5.09, N 23.53; found C 37.99, H 4.95, N 22.59. $E_{1/2}$ (CH_3CN) 0.70 V vs. SCE (E_{pc} at 0.63 V, E_{pa} at 0.77 V).

Syntheses of $[Cu(Pz_2CPh_2)_2]CuCl_2$ (7) and $Cu(Pz_2CPh_2)Cl_2$ (8): In a dry box with a nitrogen atmosphere, CuCl (0.052 g, 0.52 mmol) and **1** (0.155 g, 0.52 mmol) were combined in CH_3CN (10 mL). The resultant clear solution was left to stir for 6 hours. Slow evaporation of the reaction solution yielded clear crystals of compound **7** suitable for single-crystal X-ray diffraction (quantitative yield). The crystal structure was solved in the *Cc* space group. The literature reports that this space group can be problematic[35,36] so attempts were also made to solve the structure using the suggested *C*2/*c* space group, which incorporates a center of symmetry. However, refinement using *C*2/*c* was poor (R_1 ca. 20 %) as compared to *Cc* (R_1 = 3.83 %) and it was determined that the correct space group for structural elucidation was, in fact, *Cc*. In addition, the structure solved using *Cc* has C−C phenyl ring bond lengths [1.373(5)−1.404(4) Å] closer to the literature value of 1.397 Å, as compared to those for the elucidated structure in *C*2/*c* (1.305−1.434 Å). ES MS (+ ion, MeOH) 663.3 *m*/*z* [M − $CuCl_2$]. $C_{38}H_{32}Cl_2Cu_2N_8$ (798.70): calcd. C 57.14, H 4.05, N 14.02; found C 57.22, H 3.91, N 14.22.

A portion of compound **7** was redissolved in CH_3CN and exposed to air. The white solution of **7** gradually turned green over a 12 hour period. Crystals of the final oxidized green product (**8**) were grown by layering CH_2Cl_2 and hexane at room temperature. Additionally, compound **8** was synthesized by the reaction of $CuCl_2$ (0.158 g, 1.1 mmol) in THF (5 mL) with a THF solution of **1** (0.352 g, 1.2 mmol). Upon combining the two solutions a green precipitate formed immediately. The precipitate was removed via filtration and washed with additional THF (59.9 % yield). UV/Vis (CH_2Cl_2), λ (ε) = 417.0 nm (644 $M^{-1}cm^{-1}$), 677.0 (86 $M^{-1}cm^{-1}$). ES MS (+ ion, $CHCl_3$) 398.2 *m*/*z* [M − Cl]. $C_{19}H_{16}Cl_2CuN_4$ (434.80): calcd. C 52.47, H 3.72, N 12.88; found C 52.10, H 3.72, N 12.37. $E_{1/2}$ (CH_3CN) 0.37 V vs. SCE (E_{pc} at 0.26 V, E_{pa} at 0.47 V).

X-ray crystallography: X-ray intensity data were measured at 100 K (Bruker KRYO-FLEX) on a Bruker SMART APEX CCD-based X-ray diffractometer system equipped with a Mo-target X-ray tube (λ = 0.71073 Å) operated at 2000 watts power. Crystals were mounted on a cryoloop using Paratone N-Exxon oil and placed under a stream of nitrogen. The detector was placed at a distance of 5.009 cm from the crystals. Analyses of the data sets showed negligible decay during data collection. The data were corrected for absorption with the SADABS program. The structures were refined using the Bruker SHELXTL Software Package (Version 6.1), and were solved by direct methods until the final anisotropic full-matrix, least-squares refinement of F^2 converged.[37] Experimental details for all of the structures are provided in Table 3.

EPR experiments on compounds were carried out using a Bruker EMX X-band CW-EPR spectrometer consisting of an ER 041XG microwave bridge and a TE102 cavity coupled with a BVT 3000 nitrogen gas temperature controller (temperature stability of 0.2 K). EPR spectra were acquired by taking a 168 s field-swept scan with the center field set to 3200 G, a sweep width of 2000 G, a microwave frequency of 9.42 GHz, the modulation frequency was set to 100 kHz, and a modulations amplitude of 10.0 G. The spectra were acquired at a temperature of 120 K. The samples were dissolved in methanol to a final concentration of 1 mg/mL and transferred to 4 mm 707-SQ-250M fused quartz EPR tubes (Wilmad, Buena, NJ).

Cyclic voltammetry measurements were carried out on compounds **4**, **5**, **6** and **8** using a BAS 100B/W electrochemical workstation from Bioanalytical Systems, Inc. in West Lafayette, Indiana. HPLC grade acetonitrile (< 0.02 % H_2O) was used without further purification. A three-electrode setup with a platinum working electrode, a platinum wire electrode, and a saturated calomel reference elec-

trode was employed. Copper complexes were prepared at 1 mM concentration using 0.1 M tetrabutylammonium tetrafluoroborate as the supporting electrolyte in CH_3CN. A scan rate of 50 mV/s afforded optimal reversible behavior. Solutions were degassed with nitrogen prior to use and all experiments were run under a blanket of inert gas.

CCDC-216892 to -216898 contain the supplementary crystallographic data for this paper. These data can be obtained free of charge at www.ccdc.cam.ad.uk/conts/retrieving.html [or from the Cambridge Crystllographic Data Centre, 12 Union Road, Cambridge CB21EZ, UK; Fax: (internat.) + 44-1223/336-033; E-mail: deposit@ccdc.cam.ac.uk].

Acknowledgments

J. L. S. acknowledges the GAANN fellowship for financial support. C. J. Z. acknowledges the University of Akron for a faculty research grant (FRG-1524). We also wish to acknowledge NSF Grant CHE-0116041 for funds used to purchase the Bruker-Nonius diffractometer and the Kresge Foundation and donors to the Kresge Challenge Program at the University of Akron for funds used to purchase the NMR instrument used in this work.

[1] S. Trofimenko, J. C. Calabrese, J. Domaille, J. S. Thompson, *Inorg. Chem.* **1989**, *28*, 1091−1101.
[2] A. L. Rheingold, L. N. Zakharov, S. Trofimenko, *Inorg. Chem.* **2003**, *42*, 827−833.
[3] S. Trofimenko, J. C. Calabrese, J. S. Thompson, *Inorg. Chem.* **1987**, *26*, 1507−1514.
[4] M. Ruf, H. Vahrenkamp, *Inorg. Chem.* **1996**, *35*, 6571−6578.
[5] H. Vahrenkamp, *Acc. Chem. Res.* **1999**, *32*, 589−596.
[6] H. Boerzel, M. Koeckert, W. Bu, B. Spingler, S. J. Lippard, *Inorg. Chem.* **2003**, *42*, 1604−1615.
[7] N. Kitajima, *Adv. Inorg. Chem.* vol. 39 (Synthetic approach to the structure and function of copper proteins) (Ed.: A. G. Sykes), Academic Press, New York, **1992**, 1−77.
[8] N. Kitajima, K. Fujisawa, M. Tanaka, Y. Moro-oka, *J. Am. Chem. Soc.* **1992**, *114*, 9232−9233.
[9] D. Qiu, L. Kilpatrick, N. Kitajima, T. G. Spiro, *J. Am. Chem. Soc.* **1994**, *116*, 2585−2590.
[10] D. W. Randall, S. Debeer George, B. Hedman, K. O. Hodgson, K. Fujisawa, E. I. Solomon, *J. Am. Chem. Soc.* **2000**, *122*, 11620−11631.
[11] N. Kitajima, K. Fujisawa, C. Fujimoto, Y. Moro-oka, S. Hashimoto, T. Kitagawa, K. Toriumi, K. Tatsumi, A. Nakamura, *J. Am. Chem. Soc.* **1992**, *114*, 1277−1291.
[12] E. T. Adman, *Adv. Protein Chem.* **1991**, *42*, 144−197.
[13] E. I. Solomon, M. J. Baldwin, M. D. Lowery, *Chem. Rev.* **1992**, *92*, 521−542.
[14] S. Mandal, G. Das, R. Singh, R. Shukla, P. K. Bharadwaj, *Coord. Chem. Rev.* **1997**, *160*, 191−235.
[15] K. Shiu, L. Yeh, S. Peng, M. Cheng, *J. Organomet. Chem.* **1993**, *460*, 203−211.
[16] S. Tsuji, D. C. Swenson, R. F. Jordan, *Organometallics* **1999**, *18*, 4758−4764.
[17] S. Trofimenko, *J. Am. Chem. Soc.* **1970**, *92*, 5118−5126.
[18] M. A. Mesubi, F. O. Anumba, *Transition Met. Chem.* **1985**, *10*, 5−8.
[19] C. Pettinari, G. G. Lobbia, G. Sclavi, D. Leonesi, *Polyhedron* **1995**, *14*, 1709−1723.
[20] C. Pettinari, F. Marchetti, A. Cingolani, D. Leonesi, M. Colapietro, S. Margadonna, *Polyhedron* **1998**, *17*, 4145−4154.
[21] C. Pettinari, R. Pettinari, M. Pellei, G. G. Lobbia, *Polyhedron* **1999**, *18*, 1941−1951.
[22] J. Reedijk, J. Verbiest, *Transition Met. Chem.* **1979**, *4*, 239−243.
[23] K. Flinzner, A. F. Stassen, A. M. Mills, A. L. Spek, J. G. Haasnoot, J. Reedijk, *Eur. J. Inorg. Chem.* **2003**, 671−677.
[24] A. M. Schuitema, M. Engelen, I. A. Koval, S. Gorter, W. L. Driessen, J. Reedijk, *Inorg. Chim. Acta* **2001**, *324*, 57−64.
[25] S. Knapp, T. P. Keenan, X. Zhang, R. Fikar, J. A. Potenza, H. J. Schugar, *J. Am. Chem. Soc.* **1990**, *112*, 3452−3464.
[26] D. Martini, M. Pellei, C. Pettinari, B. W. Skelton, A. White, *Inorg. Chim. Acta* **2002**, *333*, 72−82.
[27] M. K. Ehlert, S. J. Rettig, A. Storr, R. C. Thompson, J. Trotter, *Can. J. Chem.* **1989**, *67*, 1970−1974.
[28] J. L. Schneider, V. G. Young, W. B. Tolman, *Inorg. Chem.* **2001**, *40*, 165−168.
[29] C. H. Dungan, W. Maringgele, A. Meller, K. Niedenzu, H. Nöth, J. Serwatowska, J. Serwatowska, *Inorg. Chem.* **1991**, *30*, 4799−4806.
[30] H. Yokoi, A. W. Addison, *Inorg. Chem.* **1977**, *16*, 1341−1349.
[31] J. S. Thompson, T. J. Marks, J. A. Ibers, *J. Am. Chem. Soc.* **1979**, *101*, 4180−4192.
[32] W. B. Tolman, *Inorg. Chem.* **1991**, *30*, 4880−4882.
[33] P. L. Holland, W. B. Tolman, *J. Am. Chem. Soc.* **1999**, *121*, 7270−7271.
[34] B. Kozlevčar, P. Gamez, R. Gelder, W. L. Driessen, J. Reedijk, *Eur. J. Inorg. Chem.* **2003**, 47−50.
[35] R. E. Marsh, *Acta Crystallogr., Sect. B* **1997**, *53*, 317−322.
[36] F. H. Herbstein, R. E. Marsh, *Acta Crystallogr., Sect. B* **1998**, *54*, 677−686.
[37] G. M. Sheldrick, *SHELXTL, Crystallographic Software Package*, version 6.10; Bruker-AXS: Madison, WI, 2000.

Received August 7, 2003
Early View Article
Published Online January 28, 2004

